Myocardial Mechanics in Left Ventricular Noncompaction Cardiomyopathy

Subjects: Cardiac & Cardiovascular Systems

Contributor: Attila Nemes

Left ventricular (LV) non-compaction (LVNC) is a rare genetic cardiomyopathy due to abnormal intra-uterine arrest of compaction of the myocardial fibers during endomyocardial embryogenesis. Due to the partial or complete absence of LV compaction, the structure of the LV wall shows characteristic abnormalities, including a thin compacted epicardium and a thick non-compacted endocardium with prominent trabeculations and deep intertrabecular recesses. LVNC is frequently associated with chronic heart failure, life-threatening ventricular arrhythmias, and systemic embolic events.

left ventricular | non-compaction | cardiomyopathy | cardiac mechanics

1. Noncompaction Cardiomyopathy

Left ventricular (LV) noncompaction (NC) cardiomyopathy (NCCM) or spongiform cardiomyopathy is a rare disorder due to abnormal intra-uterine arrest of compaction of the myocardial fibers during endomyocardial embryogenesis between the fifth and eighth weeks of gestation [1][2][3][4]. In a significant number of LVNC cases, mutations of genes encoding sarcomeric or cytoskeletal proteins have been shown, but an acquired case of peripartum evolution of the acquired LVNC syndrome has also been demonstrated [5]. The pathology was first detected by Engberding and Bender in 1984, but at that time it was called ventricular sinusoidosis based on the echocardiographic images seen [2]. Later, after clarifying the origin of the disease, the term “LV noncompaction” (LVNC) began to be used. Normally, LV compaction occurs from the epicardium to the endocardium and from the basal part of the LV to the apex.

Due to the partial or complete absence of LV compaction, the structure of the LV wall shows characteristic abnormalities, including a thin compacted epicardium and a thick non-compacted endocardium with prominent trabeculations and deep intertrabecular recesses. Due to the rarity of the disease, currently only limited data are available on myocardial mechanics, valvular abnormalities, and vascular remodeling in a larger group of NCCM patients. Therefore, the present paper aimed to summarize these LVNC-associated abnormalities in a series of patients. Literature data of isolated RV [6]. Case reports, rare coincidences, and associations of LVNC and other disorders, such as congenital, atherosclerotic, secondary valvular, or other diseases, are not included. Arrhythmologic and thromboembolic consequences of LVNC were also not analyzed. There is a special group of patients in whom LVNC and coronary artery disease are present at the same time, and it is not known whether regional wall motion abnormalities are caused by the coronary artery disease or the noncompaction of the myocardium in most cases [7].

2. Cardiovascular Imaging and Criteria

During the last few years, cardiac computed tomography and cardiac magnetic resonance imaging (cMRI) have become an integral part of routine clinical practice due to the advances in imaging and computing software and hardware. In addition, echocardiography has developed significantly, and new modalities have appeared and become part of the everyday practice. As a result, more detailed volumetric and functional chamber quantifications, analysis of myocardial mechanics and valvular morphology and function, and more detailed assessments of vascular function have become clinically available. For the diagnosis of NCCM, several echocardiographic and cMRI-derived criteria are used [8]. The most important ones are detailed below:

Echocardiographic criteria (**Figure 1**):

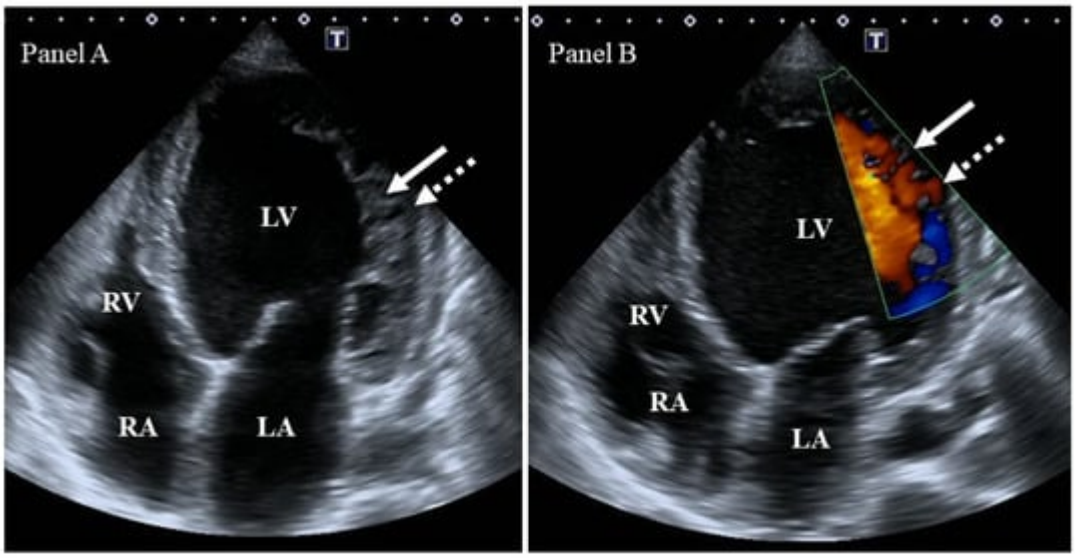

Figure 1. Two-dimensional grey-scale image (**Panel A**) and Doppler evidence (**Panel B**) of left ventricular (LV) noncompaction demonstrating LV lateral wall trabeculation (white arrows) and sinuses (dashed white arrows). Abbreviations: LV = left ventricle, LA = left atrium, RV = right ventricle, RA = right atrium.

- Chin's criterion is the earliest and simplest criterion: The distance between the epicardial surface and the trough of the trabeculation divided by the distance between the epicardial surface and the peak of the trabeculum measured at the apex of the LV in parasternal short-axis and apical views is ≤0.5 [3].

- Jenni's criterion is more complicated and takes into account a number of other factors: (I) the presence of a two-layer myocardial structure with a thin compacted and a thicker noncompacted myocardium, (II) the ratio of noncompacted to compacted myocardium > 2 at the end-systole, (III) the absence of coexisting cardiac structural abnormalities, and (IV) excessive prominent trabeculations and deep intertrabecular recesses filled with intraventricular blood with color Doppler imaging. Parameters are measured in parasternal short-axis views [4].

- Stollberger's criterion is a simplified criterion that is closer to the clinical routine: (I) the presence of >3 trabeculations located apically to the papillary muscles in parasternal short-axis and apical views, within a distinct two-layered myocardium in the end-systole, and (II) perfusion of intertrabecular recesses with either color Doppler or echocardiographic contrast imaging in the end-diastole [9].

cMRI criteria:

- Petersen's criterion is simple, as it aims to assess the noncompacted/compacted myocardial ratio, ideally with a ratio > 2.3 in the end-diastole, excluding the LV apex from the measurement, as the compacted myocardium is physiologically thinner [10].

- Jacquier's criterion aims to assess trabecular LV mass, and a value > 20% of global LV mass in the end-diastole is diagnostic [11].

- Grothoff's criterion is more complicated: (I) LV myocardial mass index of the noncompacted tissue ('a') >15 g/m^2, (II) 'a' as a percentage of total LV myocardial mass index >25%, and (III) increased trabeculation in LV basal segments and a noncompacted/compacted ratio ≥3:1 measured in the end-diastole on the short axis [12].

3. The Left Heart and the Aorta

3.1. Left Ventricle

3.1.1. Under Healthy Circumstances

The LV is an egg- or bullet-shaped cardiac chamber. Muscle bands and papillary muscles limit obtaining the optimal contours in order to enable accurate measurements. In healthy subjects, during systole, the mitral valve (MV) closes and the aortic valve (AV) opens, allowing blood flow from the LV to the aorta, whereas during diastole, blood flows into the LV from the left atrium (LA) across the open MV. During this phase of the cardiac cycle, the AV is closed. In the LV, there are subepicardial fibers running in a left-handed direction, fibers in the mid-layer running circumferentially, and subendocardial fibers running in a right-handed direction [13][14]. Movements of the LV wall follow a 3D pattern, including radial thinning/thickening, longitudinal lengthening/shortening, and circumferential widening/narrowing during the cardiac cycle. This myocardial deformation in 3D can be represented by echocardiographic strains: simple unidimensional/unidirectional radial (LV-RS), longitudinal (LV-LS), and circumferential (LV-CS) strains, with the combination of them being area strain (LV-AS, combination of LV-LS and LV-CS) or 3D strain (LV-3DS, combination of all strains) [13][15][16][17][18]. Furthermore, these movements of the LV wall are not independent; the basal regions of the LV rotate in a clockwise direction during systole, whereas the apex of the LV moves in the opposite counterclockwise direction under healthy circumstances. These opposite basal and apical rotations result in an LV twist, which leads to the LV wringing during systole. In diastole, LV untwisting is seen, during which the basal and apical LV regions move in opposite directions compared to the movements during systole [13][14][19] (**Figure 2**).

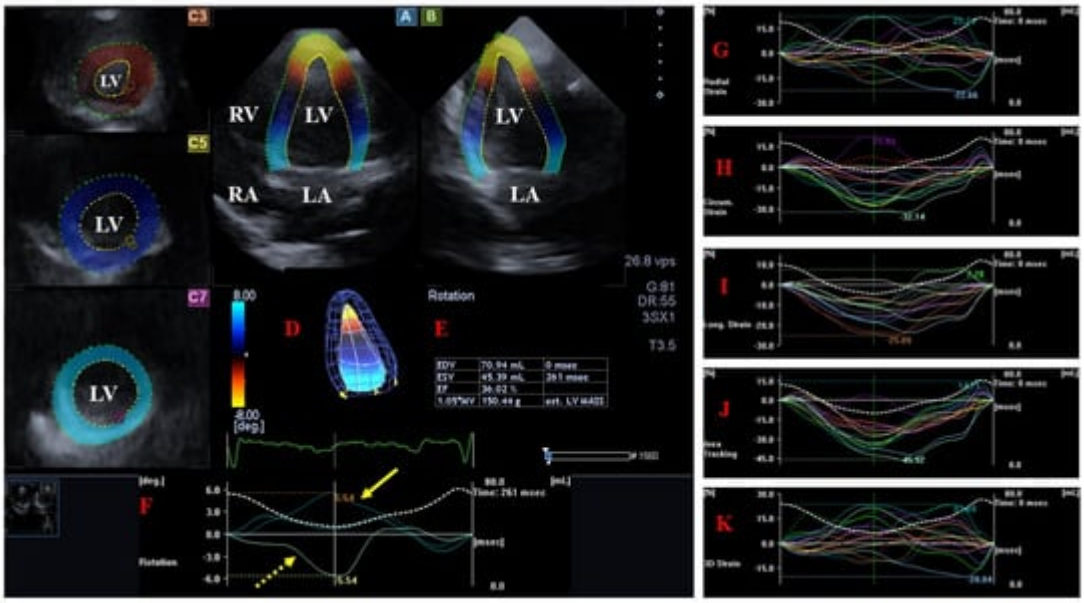

Figure 2. Evaluation of the left ventricle by three-dimensional (3D) speckle−tracking echocardiography. Following the acquisition of a 3D echocardiographic dataset and by using a dedicated vendor-provided software, several views are produced automatically: longitudinal apical four-chamber (**A**) and two-chamber (**B**) views and short-axis views at the apical (**C3**), midventricular (**C5**), and basal (**C7**) LV regions. The 3D LV model (**D**), calculated LV volumes and ejection fraction (**E**), and apical (yellow arrow) and basal (yellow dashed arrow) LV rotations (**F**), together with time–LV global (white curve) and segmental (colored curves) radial (**G**), circumferential (**H**), longitudinal (**I**), area (**J**), and 3D (**K**) strain curves with a time–LV volume change curve (dashed white curve), are demonstrated. The image presents a patient with reduced LV function (decreased LV ejection function) and normally directed LV rotational mechanics with reduced counterclockwise apical (yellow arrow) and preserved clockwise basal (dashed yellow arrow) LV rotations. Abbreviations: LV = left ventricle, LA = left atrium, RV = right ventricle, RA = right atrium, EDV = LV end-diastolic volume, ESV = LV end-systolic volume, EF = LV ejection fraction, MASS = LV muscle mass.

3.1.2. In Noncompaction Cardiomyopathy

LV Structure, Volumes, and Function

In an early study, the extension of NC myocardium was predominantly seen at the apex (72%), with an LV ejection fraction (EF) < 50% in 83% of the patients. Hypokinesis was observed in both noncompacted and compacted segments [20]. In another pool of LVNC patients, 60% of the patients were in New York Heart Association (NYHA) functional class III/IV and 79% had systolic dysfunction (LV-EF < 50%). A dilated left heart with systolic dysfunction was found to be one of the predictors of an adverse outcome [21]. In another pool of isolated sub-Saharan African LVNC patients, 63% of the subjects had NYHA functional class II, and heart failure due to systolic dysfunction was the most common clinical presentation (98%). The LV end-diastolic diameter was dilated and LV-EF was impaired. Common sites of noncompaction were the apical (100%), midinferior (74.1%), and midlateral (64.8%) regions [22].

Wall motion abnormalities were present in the majority of the compacted LV segments in LVNC patients [23][24][25]. The wall motion score (WMS) index was markedly abnormal in the compacted LV segments of LVNC patients but significantly less abnormal compared to the noncompacted segments [26]. In a recent real-time 3D echocardiographic study, contributions of compacted and noncompacted segments to global LV systolic dysfunction were examined in LVNC. Noncompacted and compacted LV segments had comparable increased regional volumes and reduced systolic function, suggesting that systolic LV dysfunction observed in LVNC is not confined to noncompacted LV segments [26]. There was an inverse correlation between the noncompacted area and LV-EF, suggesting that noncompaction itself contributes to LV dysfunction [27]. In contrast, paradoxical contributions of noncompacted vs. compacted segments to global LV dysfunction were found in another study: Relatively less impairment in the WMS index in case of the noncompacted segments was seen compared to the compacted value of the LV segments [28]. Moreover, a strong correlation was found between systolic and diastolic dysfunction in LVNC by tissue Doppler imaging [29]. No relationship between LV radial wall motion and longitudinal velocity and the extent and severity of NCCM could be demonstrated [30].

LV Strains

Compared with controls, patients with LVNC with preserved LV-EF had similar LV systolic function and chamber dimensions but a larger mass and greater relative wall thickness, more abnormal LV geometry, and decreased global LV-LS [31]. In other studies, global LV-CS and LV-RS proved to be reduced in the same population [32][33]. Although LV trabecular muscle mass was very different between men and women, no disease-related strain differences were found between men and women [32]. In a further study, patients with LVNC with normal LV-EF showed impaired global LV-RS, LV-CS, and LV-LS. The extent of excessive trabeculation was higher in LVNC compared to controls, and this value positively correlated with LV end-diastolic and end-systolic volume indices, and stroke volume index but negatively correlated with global LV-RS and LV-CS [34].

It was also demonstrated in LVNC patients that global LV-LS was reduced regardless of LV-EF [35][36] and that global LV-LS and QRS duration were associated with LV-EF in LVNC [37]. Global and regional LV-LS and LV-CS were impaired in LVNC, and apical peak LV-CS was strongly associated with cardiovascular events [38]. The myocardial strain of the cardiac apex and endocardium was significantly lower than that of the cardiac base and epicardium, respectively. Myocardial strain reduction was more significant in LVNC patients with focal myocardial fibrosis [39]. LVNC patients with heart failure (HF) with preserved LV-EF have diffuse fibrosis, which is more extensive at the apical level, explaining the decrease in apical deformation. Lower transmural and base-to-apex deformation gradients support the sequence of myocardial maturation failure [40]. The strain values changed as LV-EF decreased, but the LVNC-specific LV strain pattern could not be detected [41]. In LVNC patients with severe HF, LV-EF increased, but LV volumes did not change during the follow-up after cardiac resynchronization therapy. A total of 33% of patients proved to be respondent, with a reduction in inter-ventricular, longitudinal, and radial intra-ventricular dyssynchrony [42]. The presence of myocardial ischemia in NCCM patients is associated with LV dilation and worse LV function represented by LV-EF and global LV-LS [43].

All 3DSTE-derived strains proved to be significantly decreased in all segments of LVNC patients compared to segments of controls. However, LV-RS and LV-3DS showed further reduction in noncompacted segments compared to compacted segments (results from the MAGYAR-Path Study) [44]. This was partly confirmed when severely diminished myocardial efficiency was found in LVNC, and LV function seemed to depend mainly on the compact myocardial wall layer [45]. The impairment of all strains correlated well with the extent of the non-compacted myocardium as well [46]. In contrast, lower regional deformation values in compacted segments compared to noncompacted segments with relatively preserved apical deformation compared to basal segments were found in another study on LVNC [47].

Beyond the above fact, a significant decrease in LV-EF, fractional shortening, E/E', and global LV strains could be detected in the relatives of the patients compared to healthy volunteers [48]. Moreover, carriers of multiple genetic variants had a lower LV-EF and cardiac index, increased LV fibrosis, and reduced global LV-CS in LVNC [49].

In addition to studies conducted in adults [50], extensive studies have also been carried out in children. LVNC in pediatric patients was associated with LV enlargement and impaired LV systolic function, represented by lower LV-EF and LV strains [51]. In another study, LV myocardial deformation was found to be decreased in longitudinal and circumferential dimensions by 2DSTE in NCCM children [52]. In LVNC children with normal LV-EF, LV-LS and LV-CS values were reduced [53]. In a number of studies, impairment of LV-EF, end-diastolic dimension, or LV posterior wall compaction and decreased LV strains were associated with adverse outcomes in children [54][55]. Global and segmental LV-RS, LV-CS, and LV-LS were decreased in pediatric patients with LVNC [51][56], and the lowest segmental values were found in those with adverse outcomes compared with those with benign outcomes [56].

Naturally, the possible use of LV strains in differential diagnosis was also raised. Global LV-LS showed significant differences between LVNC and dilated cardiomyopathy (DCM) [57][58]. The base–apex longitudinal gradient of the strain appears as a valuable additive tool for distinguishing LVNC from DCM [58]. Regarding the early findings, a special regional deformation pattern with preserved deformation in basal segments of LVNC can help to differentiate LVNC from DCM as well [59]. In contrast, LV volumes and global LV-LS and LV-CS were similar in DCM and in LVNC, but the trabeculated and papillary muscle index was higher and apical LV-CS was significantly lower in LVNC than in DCM. These minor alterations might be due to the morphological characteristics of LVNC with a trabeculated apical region [60]. In another study, LV segmental strain analysis revealed that basal LV-CS was lower in DCM than in LVNC. In correspondence with previous findings, both median and apical LV-LS were lower in LVNC than in DCM; moreover, apical LS was the most effective in distinguishing LVNC from DCM [61]. In an early study examining the differentiation of LVNC and hypertrophic cardiomyopathy (HCM), an increased number of trabeculations, a thinner maximal wall thickness, and a lower LV-EF with homogeneously reduced myocardial function were found in LVNC, whereas an apical-to-basal gradient with relatively preserved apical function was present in HCM [62]. LVNC showed a more significant reduction in LV-LS in the apical region compared to patients with HCM, suggesting an abnormality of development in these regions [63].

LVNC patients with mitral valve (MV) regurgitation had more severe morphological and functional LV changes [64]. In another study, LVNC patients with MV regurgitation showed significant deterioration in LV myocardial strains and

impaired LV geometry and function, including lower LV-EF and greater LV end-systolic volume and LV mass compared to LVNC patients without MV regurgitation. Moreover, the incidence of adverse outcomes may be related to the degree of MV regurgitation in these cases [65].

LV Rotational Mechanics

In a recent study, LV rotational parameters of healthy adolescent athletes meeting Jenni's criteria for LVNC were not worse compared to those who did not meet the criteria [66]. LV twist was found to be significantly reduced in young patients with LVNC compared with controls and those with LV hypertrabeculation, and reduced LV twist was an independent predictor of LVNC [67]. In contrast, the peak LV twist values were comparable between LVNC patients and controls [31]. In another study, the rotation of basal LV segments was reduced and the rotation of apical LV segments was much lower, resulting in reduced LV twist [38][68]. Apical LV rotation and net LV twist were lower in NCCM/LVNC patients compared to controls [36][46][48], but both basal and apical LV rotations were reduced in patients with LVNC with LV-EF < 50% [35][36]. The impairment of LV twist parameters correlates well with the extent of the non-compacted myocardium [46]. Upon comparing patients and their relatives, despite no difference being found in the patients' relatives, a decreasing pattern in rotation values was found [48]. LV twist was associated with cardiovascular events [38]. There was no difference in the rotational pattern between DCM and LVNC, and both healthy and patient populations showed heterogeneous rotational patterns [60].

LV Rigid Body Rotation

In some cases, both basal and apical LV segments move in the same direction, resulting in an absence of LV twist. NCCM/LVNC is the most examined disorder in which a near absence of LV twist, known as LV rigid body rotation (LV-RBR), was found in 26% to 100% of cases [31][35][41][48][63][67][68][69][70][71][72]. It was suggested early on that LV-RBR may be a new sensitive and specific, objective and quantitative, functional diagnostic criterion for NCCM [69]. LV-RBR had 88% specificity and 78% sensitivity in differentiating NCCM from LV hypertrabeculation [70]. Similar results were found in children, in whom LV-RBR was present in 56% of NCCM patients and in 4% of subjects with hypertrabeculation [67]. LV-RBR was present in 100% [69], 88% [70], 57% [35], 56% [67], 53% [48][68], 50% [63], 39% [71], and 26% of cases [38] in a series of NCCM/LVNC patients. LVNC patients with LV-RBR showed worse NYHA functional status but similar signs of remodeling, LV-EF, and strain values compared to those with LVNC and normally directed LV rotational mechanics [68]. The presence and direction of LV-RBR seemed to be related to LV-EF: Patients with lower LV-EF (<50%) had higher rates of clockwise LV-RBR (39%), whereas subjects with LV-EF > 50% had a ratio of 26% of counterclockwise LV-RBR [41]. In another study, the ratio of LV-RBR proved to be 92.3% vs. 26.7% in the same subgroups, respectively [35]. Patients with reverse apical rotation (clockwise LV-RBR) had lower LV-LS but similar LV-EF compared with patients without reverse apical rotation [71]. In most cases, LV-RBR proved to be clockwise oriented in NCCM [48][67][68][69][70][71]. When NCCM patients and their first-degree relatives were compared, 53% and 30% showed LV-RBR with the same ratio of a dominantly clockwise vs. counterclockwise pattern, respectively [48]. The prevalence of LV-RBR was significantly increased (57% vs. 14%, $p = 0.05$) in the LVNC population compared to controls [31].

3.2. Left Atrium

3.2.1. Under Healthy Circumstances

The LA has circumferential (e.g., interatrial band, located at the base) and longitudinal (e.g., septoatrial band, located parietally) muscle bands. The rim of the oval fossa has an important role, because the other main muscles of the atrium are attached to it. The LA has a significant role in modulating the filling of the LV. It serves as a reservoir for pulmonary venous flow during LV systole and as a conduit for pulmonary venous return during early LV diastole, as well as a booster pump that enhances ventricular filling during late LV diastole. The volume of the LA is maximal at end-systole just before MV opening and is minimal at end-diastole when the MV closes, and there is a pre-atrial contraction volume directly before atrial systole. Several stroke volumes and emptying fractions could be calculated as functional properties from LA volumes to evaluate all phases of LA function. The Frank–Starling mechanism applies to the LA, meaning that an increase in LA wall contractility can be detected in response to increased LA preload up to a point, beyond which this correlation disappears (**Figure 3**) [73][74][75].

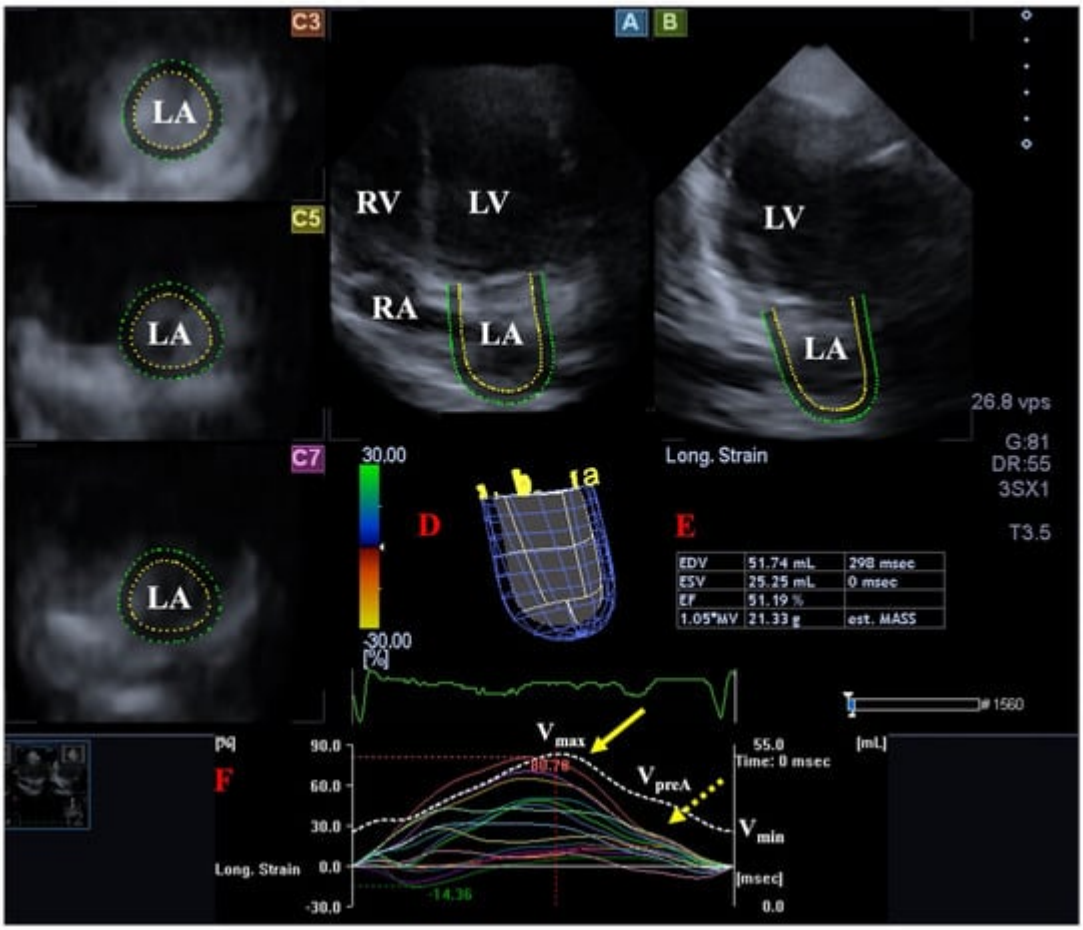

Figure 3. Evaluation of the left atrium (LA) by three-dimensional (3D) speckle-tracking echocardiography. Following acquisition of a 3D echocardiographic dataset and by using a dedicated vendor-provided software, several views are produced automatically: Longitudinal apical four-chamber (**A**) and two-chamber (**B**) views, together with short-axis views at the basal (**C3**), midatrial (**C5**), and superior (**C7**) LA regions, are demonstrated. A virtual 3D LA cast (**D**), together with calculated LA volumes (**E**) and time–LA global (white curve) and segmental (colored curves) longitudinal (**F**) strain curves with a time–LA volume change curve (dashed white curve), are also

demonstrated. The yellow arrow represents peak LA strains, whereas the yellow dashed arrow represents LA strains at atrial contraction. Abbreviations: LV = left ventricle, LA = left atrium, RV = right ventricle, RA = right atrium, EDV = end-diastolic volume, ESV = end-systolic volume, EF = ejection fraction, MASS = LA muscle mass, Vmax = minimum end-systolic LA volume, VpreA = early diastolic LA volume before atrial contraction, Vmin = end-diastolic minimum LA volume.

3.2.2. In Noncompaction Cardiomyopathy

In LVNC, signs of LA remodeling [31] and a larger LA diameter were detected [35][76], which was related to a higher risk of thromboembolism in LVNC patients, suggesting that it may be a useful predictor for thrombotic risk stratification [76]. LA ejection force as a characteristic of LA systolic function was found to be increased in LVNC patients compared to healthy individuals, suggesting a compensation of LA work against the dysfunctional LV [77]. Significantly greater LA volumes, smaller LA emptying fractions, and reduced peak global LA-RS, LA-CS, and LA-AS representing systolic function were present in LVNC patients with reduced LV-EF, as assessed by 3DSTE in the MAGYAR-Path Study [78]. In a recent study, the LA reservoir strain was an independent predictor for high-risk HF events in LVNC patients, and LV-GLS was an independent determinant of the LA reservoir strain [79]. Compared to negative genotype LVNC patients, subjects with a positive genotype had a larger LA volume, a lower LA reservoir, and booster pump strains. Moreover, LA volume can be used to discriminate patients with a positive genotype, as well as those with multiple genetic mutations [49].

3.3. Mitral Valve

3.3.1. Under Healthy Circumstances

The MV or left bicuspid atrioventricular valve is a saddle-shaped structure in 3D with a dynamic motion during the cardiac cycle. The MV is composed of the fibrous mitral annulus (MA), the anterior and the posterior leaflets, the tendineal chords, and the papillary muscles. The MV allows normal blood flow from the LA to the LV during diastole and prevents blood backflow (mitral regurgitation) from the LV to the LA during systole. Timely contraction of adjacent LA and LV areas is necessary for proper contraction of MV under healthy circumstances (**Figure 4**) [80][81][82].

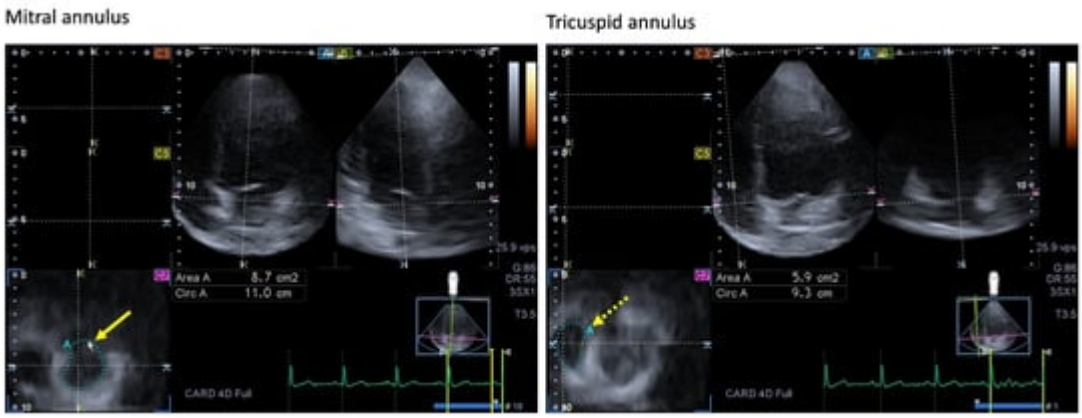

Figure 4. Images showing two-dimensionally projected views of the mitral (MA) and tricuspid (TA) annuli as assessed by three-dimensional (3D) speckle-tracking echocardiography. After the acquisition of the 3D echocardiographic dataset, the following views were produced: Apical four-chamber (**A**) and two-chamber views (**B**) and a cross-sectional view at the level of the MA/TA were optimized in apical four- and two-chamber views (**C7**). The yellow arrow represents the two-dimensional projection of the MA plane, whereas the yellow dashed arrow represents the two-dimensional projection of the TA plane. Abbreviations: LA = left atrium, LV = left ventricle, RA = right atrium, RV = right ventricle, Area = MA/TA area, Circ = MA/TA perimeter.

3.3.2. In Noncompaction Cardiomyopathy

MA was dilated and functionally impaired in LVNC patients with impaired LV systolic function with a higher incidence and severity of mitral regurgitation. The number of non-compacted segments did not correlate with MA dimensions and functional properties. No, mild, and moderate to severe MV regurgitation could be detected in 45%, 35%, and 20% of subjects, respectively [83]. In the MAGYAR-Path Study, 33% − 33% of patients showed regurgitation of grades 1 and 2 MV [84]. In other studies, 48.2% and 78% of the subjects showed MV regurgitation [64][85].

3.4. Aortic Valve

3.4.1. Under Healthy Circumstances

The aortic valve (AV) separates the LV outflow tract from the ascending aorta and has three semilunar thin leaflets ensuring one-way blood flow towards the systemic circulation. It opens during ventricular systole and closes during ventricular diastole in order to prevent blood flowing from the ascending aorta backwards into the LV [86].

3.4.2. In Noncompaction Cardiomyopathy

In pools of patients with bicuspid AV, the prevalence of associated LVNC proved to be 0.2% [87], 3.4% [88], and 11% [89]. Jenni's, Petersen's, and Fazio's LVNC criteria were associated with BAV in 10.1%, 62.0%, and 54.4% of patients, respectively. These results confirmed that BAV patients do not harbor more LVNC than the general population, and there is no evidence that they are at higher risk for the development of LVNC cardiomyopathy [90]. In a recent study, 19 out of 46 LVNC patients (41%) showed AV regurgitation [85].

3.5. Aorta

3.5.1. Under Healthy Circumstances

The aorta is the largest artery carrying blood from the LV to the body. There is a significant interaction between the cardiac chambers and the vasculature. The aorta is an elastic tube and has a significant role in regulating blood flow via the Windkessel effect. Aortic stiffness can be associated with increasing systolic blood pressure (BP) and decreasing diastolic BP, subsequently increasing LV afterload and potentially leading to LV hypertrophy, thereby impairing LV relaxation and potentially causing LV diastolic dysfunction and damaging coronary perfusion [91][92].

3.5.2. In Noncompaction Cardiomyopathy

In a cross-sectional cohort study of 109 NCCM patients, the prevalence of ascending aortic dilatation was 7%, which involved only mild dilatations and was not significantly different from an age- and sex-matched cohort of dilated cardiomyopathy patients [93]. Increased aortic stiffness with no dilation but reduced pulsatile change in aortic diameter was observed in patients with NCCM with moderate to severe HF, confirming previous findings. Changes in aortic stiffness was theorized to be due to HF-induced neurohormonal changes, not to LVNC itself [94].

4. The Right Heart and the Pulmonary Artery

4.1. Right Ventricle

4.1.1. Under Healthy Circumstances

The right ventricle (RV) is triangular in shape when viewed from the front and curves over the LV. It is crescent shaped in cross-section, with its diameter gradually increasing from the apex to the base. The RV fills from the RA during diastole through the tricuspid valve (TV) and empties into the pulmonary artery through the pulmonary valve (PV) during systole. The muscular wall of the RV, not including trabeculations, is 3–5 mm thick, resulting in a lower muscle mass compared to that of the LV (RV muscle mass is only one-fifth to one-sixth of that of the LV) [95]. The activation sequence of the RV begins in the inlet and the latest activation occurs in the outflow tract. The RV is composed of a free wall containing predominantly transverse fibers subepicardially, with deep subendocardial fibers arranged longitudinally from base to apex. The longitudinal fibers are responsible for the longitudinal shortening, during which the RV axis is shortened and the TV moves in an apical direction. The circumferential fibers play a role in the inward (radial) movement of the RV free wall (“bellows effect”). The superficial muscle fibers of the RV continue onto the LV, contributing to the interdependence of the two ventricles. The RV motion is regulated by the heart rate, the Frank–Starling mechanism, and the autonomic nervous system; the rotation and twisting motions seen in case of the LV do not play an essential role in the RV [96][97][98]. The RV is more trabeculated than the LV even in healthy subjects [99].

4.1.2. In Noncompaction Cardiomyopathy

Analysis of RV morphology in 105 LVNC patients found greater RV apical trabecular thickness among those with an LV end-systolic noncompacted-to-compacted ratio ≥ 2 compared with those with an LV end-systolic noncompacted-to-compacted ratio < 2 or the normal control group. There was no difference between the groups in relation to the RV end-diastolic noncompacted-to-compacted ratio [99]. In another study, RV systolic dysfunction was present in a non-negligible proportion of patients with isolated LVNC; LV systolic function was found to be the only variable independently related to RV systolic function [100]. LVNC was associated with increased trabeculations of the RV apex [99]. In other studies, the RV myocardium displayed more trabeculations in LVNC [101], even is children [50]. However, overlap with normal individuals was extensive, not allowing for the differentiation of patients with LVNC from controls [101]. In a pool of 54 sub-Saharan African LVNC patients, RV noncompaction occurred in 22.2% of patients with RV dilation (74.1%) and depressed RV function (59.3%) [22]. The

correlation of LV and RV trabeculation was observed only in LVNC patients with normal LV-EF, whereas LV trabeculation correlated with RV volumes in both types of LV-NC patients regardless of LV-EF. LVNC patients with reduced LV-EF had worse RV strains than patients with LVNC with normal LV-EF, but RV strains correlated with RV trabeculation predominantly in LVNC patients with reduced LV-EF [102]. Subclinical impairment of RV myocardial deformation was present even in children with LVNC [51]. The prevalence of LVNC-related clinical features was similar in patients with RV hypertrabeculation vs. RV normotrabeculation. Patients with an LVNC phenotype might have RV non-compaction with subclinical RV dysfunction and without more severe clinical features [103]. RV dysfunction was present in half of LVNC patients, seems to be a marker of advanced disease [104], and is strongly associated with adverse clinical events and prognosis [99][104][105].

4.2. Right Atrium

4.2.1. Under Healthy Circumstances

There are circumferential and longitudinal muscular bundles in the RA. The most important muscles are the terminal crest and the terminal pectinate muscles. The rim of the oval fossa has an important role, as the other main muscles of the atrium are attached to it. The RA has a complex structure and serves as a reservoir for the systemic flow return from the caval veins and the coronary sinus during systole, preparing blood to be transferred to the RV and pulmonary circulation. During early diastole, the TV opens and the RV fills passively (RA conduit function), followed by an active RA contraction at the end of diastole (“booster pump” function). Additionally, the sinus node is located in the RA, and the RA plays a role in the production of atrial natriuretic peptides regulated by RA tension and baroreceptors located in the RA wall (**Figure 5**) [106].

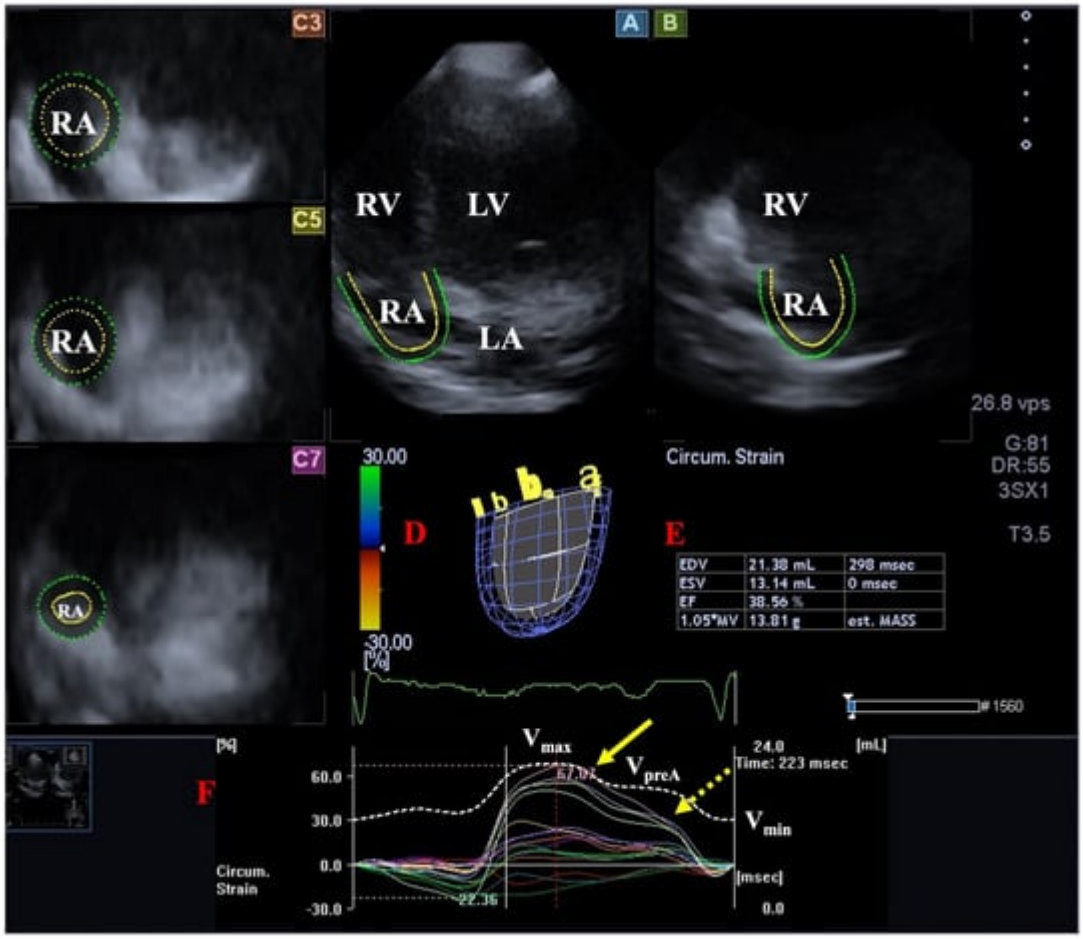

Figure 5. Evaluation of the right atrium (RA) by three-dimensional (3D) speckle-tracking echocardiography. Following acquisition of a 3D echocardiographic dataset and by using dedicated vendor-provided software, several views were produced automatically: Longitudinal apical four-chamber (**A**) and two-chamber (**B**) views and short-axis views at basal (**C3**), midatrial (**C5**), and superior (**C7**) RA levels. The 3D cast of the RA (**D**) is shown with calculated RA volumes (**E**) and time–RA global (white curve) and segmental (colored curves) longitudinal (**F**) RA strain curves together with a time–RA volume change curve (dashed white curve). The yellow arrow represents peak RA strains, whereas the yellow dashed arrow represents RA strains at atrial contraction. Abbreviations: LV = left ventricle, LA = left atrium, RV = right ventricle, RA = right atrium, EDV = end-diastolic volume, ESV = end-systolic volume, EF = ejection fraction, MASS = RA muscle mass, Vmax = minimum end-systolic RA volume, VpreA = early diastolic RA volume before atrial contraction, Vmin = end-diastolic minimum RA volume.

4.2.2. In Noncompaction Cardiomyopathy

Results from the MAGYAR-Path Study found increased cyclic 3DSTE-derived RA volumes in patients with isolated LVNC and reduced LV-EF. However, only mild RA functional alterations, including increased RA stroke volumes in systole and early diastole without RA strain abnormalities, could be detected in LVNC [107].

4.3. Tricuspid Valve

4.3.1. Under Healthy Circumstances

The right atrioventricular or tricuspid valve (TV) has a 3D, saddle-shaped, asymmetrical ellipsoid annulus, with a dynamic nature respecting the cardiac cycle, three leaflets, and a subvalvular apparatus [108]. The TV functions as a one-way valve. It opens during ventricular diastole, allowing blood flow from the RA into the RV, and it closes during ventricular systole to prevent the regurgitation of blood from the RV back into the RA (**Figure 4**).

4.3.2. In Noncompaction Cardiomyopathy

Results from the MAGYAR-Path Study confirmed that the tricuspid annulus (TA) was dilated, with preserved sphincter-like function (TA fractional area change, TAFAC and TA fractional shortening, TAFS) in patients with isolated LVNC and impaired systolic function. Longitudinal (TA plane systolic excursion, TAPSE) and sphincter-like TA movements (TAFAC, TAFS) correlated with each other. Moreover, TA dilation was associated with an increased RA volume with respect to the cardiac cycle.

4.4. Pulmonary Valve

4.4.1. Under Healthy Circumstances

The pulmonary valve (PV) is a semilunar valve that separates the RV from the pulmonary artery. The PV opens at ventricular systole and closes at ventricular diastole [109].

4.4.2. In Noncompaction Cardiomyopathy

In a recent study, 6 out of 46 LVNC patients (13%) showed PV regurgitation [85].

4.5. Pulmonary Artery

4.5.1. Under Healthy Circumstances

The pulmonary artery is a large vessel of the pulmonary system that carries deoxygenated blood from the RV to the lungs being a low-pressure, low-resistance system [98].

4.5.2. In Noncompaction Cardiomyopathy

In a pool of 54 isolated sub-Saharan African LVNC patients, pulmonary hypertension was documented in 83.3% of patients [22]. In another study, 35% of LVNC patients showed pulmonary hypertension [31].

5. Pathophysiologic Background

The genetic background of LVNC is both isolated and familial, with autosomal dominant and recessive mitochondrial gene abnormalities and X-linked inheritance [110][111][112][113]. Regarding van Waning et al., 80 genes are thought to have an influence in causing LVNC, including sarcomere genes (e.g., ACTC1, DES, etc.), transcriptional/translational genes (e.g., NKX2–5, NONO etc.), mitchondrial function genes (e.g., NNT, TAZ etc.), cytoskeletal protein genes (e.g., DMD, DTNA, etc.), cellular junction protein genes (DSP, PKP2), intracellular

trafficking genes (LAMP2, PLEKHM2), ion channel genes (HCN4, SCN5A), signal transduction genes (ALPK3, DMPK), and a protein degradation gene (MIB1) [111][112][113]. Molecular mechanisms of the specific impaired signaling pathways were established in several studies. Moreover, the inhibition of signaling and genome correction of certain mutations were sufficient as well, suggesting that the application of gene-editing techniques can have a role in the diagnosis and maybe in the treatment of NCCM in the future [114].

Shortly, the alterations detailed above can be traced back to the LV compaction abnormalities underlying the pathology. These abnormalities can lead to various manifestations of heart failure in a significant number of cases. Abnormalities in the LV may explain atrial and valvular morphological and functional alterations, as well as the reason for being more significant on the left side of the heart than on the right side of the heart. In accordance with ventricular–arterial coupling, abnormalities in the heart and large vessels have a mutual effect on each other, explaining vascular abnormalities [1][4].

There are several animal and cell culture models of LVNC that can help identify pathways involved in ventricular noncompaction. Gene-editing technologies using certain enzymes can be used for modeling LVNC. Patient-specific induced pluripotent stem cell-derived cardiomyocytes also proved to be useful for investigating LVNC [115].

References

1. Wu, M. Mechanisms of Trabecular Formation and Specification During Cardiogenesis. Pediatr. Cardiol. 2018, 39, 1082–1089.
2. Engberding, R.; Bender, F. Identification of a rare congenital anomaly of the myocardium by two-dimensional echocardiography: Persistence of isolated myocardial sinusoids. Am. J. Cardiol. 1984, 53, 1733–1734.
3. Chin, T.K.; Perloff, J.K.; Williams, R.G.; Jue, K.; Mohrmann, R. Isolated noncompaction of left ventricular myocardium. A study of eight cases. Circulation 1990, 82, 507–513.
4. Jenni, R.; Oechslin, E.; Schneider, J.; Attenhofer Jost, C.; Kaufmann, P.A. Echocardiographic and pathoanatomical characteristics of isolated left ventricular noncompaction: A step towards classification as a distinct cardiomyopathy. Heart 2001, 86, 666–671.
5. Almeida, A.G.; Pinto, F.J. Non-compaction cardiomyopathy. Heart 2013, 99, 1535–1542.
6. Gomathi, S.B.; Makadia, N.; Ajit, S.M. An unusual case of isolated non-compacted right ventricular myocardium. Eur. J. Echocardiogr. 2008, 9, 424–425.
7. Zhu, X.; Ya, Y.; Hu, G. Left ventricular noncompaction in patients with coronary artery disease: Preliminary analysis of echocardiographic findings. J. Clin. Ultrasound 2018, 46, 475–479.
8. Rao, K.; Bhaskaran, A.; Choudhary, P.; Tan, T.C. The role of multimodality imaging in the diagnosis of left ventricular noncompaction. Eur. J. Clin. Investig. 2020, 50, e13254.

9. Stollberger, C.; Gerecke, B.; Finsterer, J.; Engberding, R. Refinement of echocardiographic criteria for left ventricular noncompaction. Int. J. Cardiol. 2013, 165, 463–467.
10. Petersen, S.E.; Selvanayagam, J.B.; Wiesmann, F.; Robson, M.D.; Francis, J.M.; Anderson, R.H.; Watkins, H.; Naubauer, S. Left ventricular non-compaction: Insights from cardiovascular magnetic resonance imaging. J. Am. Coll. Cardiol. 2005, 46, 101–105.
11. Jacquier, A.; Thuny, F.; Jop, B.; Giorgi, R.; Cohen, F.; Gaubert, J.Y.; Vidal, V.; Bartoli, J.M.; Habib, G.; Moulin, G. Measurement of trabeculated left ventricular mass using cardiac magnetic resonance imaging in the diagnosis of left ventricular non-compaction. Eur. Heart J. 2010, 31, 1098–1104.
12. Grothoff, M.; Pachowsky, M.; Hoffmann, J.; Posch, M.; Klaassen, S.; Lehmkuhl, L.; Gutberlet, M. Value of cardiovascular MR in diagnosing left ventricular non-compaction cardiomyopathy and in discriminating between other cardiomyopathies. Eur. Radiol. 2012, 22, 2699–2709.
13. Narang, A.; Addetia, K. An introduction to left ventricular strain. Curr. Opin. Cardiol. 2018, 33, 455–463.
14. Nakatani, S. Left ventricular rotation and twist: Why should we learn? J. Cardiovasc. Ultrasound 2011, 19, 1–6.
15. Ammar, K.A.; Paterick, T.E.; Khandheria, B.K.; Jan, M.F.; Kramer, C.; Umland, M.M.; Tercius, A.J.; Baratta, L.; Tajik, A.J. Myocardial mechanics: Understanding and applying three-dimensional speckle tracking echocardiography in clinical practice. Echocardiography 2012, 97, 861–872.
16. Urbano-Moral, J.A.; Patel, A.R.; Maron, M.S.; Arias-Godinez, J.A.; Pandian, N.G. Three-dimensional speckle-tracking echocardiography: Methodological aspects and clinical potential. Echocardiography 2012, 29, 997–1010.
17. Muraru, D.; Niero, A.; Rodriguez-Zanella, H.; Cherata, D.; Badano, L. Three-dimensional speckle-tracking echocardiography: Benefits and limitations of integrating myocardial mechanics with three-dimensional imaging. Cardiovasc. Diagn. Ther. 2018, 8, 101–117.
18. Gao, L.; Lin, Y.; Ji, M.; Wu, W.; Li, H.; Qian, M.; Zhang, L.; Xie, M.; Li, Y. Clinical Utility of Three-Dimensional Speckle-Tracking Echocardiography in Heart Failure. J. Clin. Med. 2022, 11, 6307.
19. Sengupta, P.P.; Tajik, A.J.; Chandrasekaran, K.; Khandheria, B.K. Twist mechanics of the left ventricle: Principles and application. JACC Cardiovasc. Imaging. 2008, 1, 366–376.
20. He, T.; Zeng, H.S.; Le, W.B.; Li, X.H.; Lu, Z.Y. Clinical characterization and outcome of patients with noncompaction of ventricular myocardium. Zhonghua Xin Xue Guan Bing Za Zhi 2007, 35, 548–551.
21. Tian, T.; Liu, Y.; Gao, L.; Wang, J.; Sun, K.; Zou, Y.; Wang, L.; Zhang, L.; Li, Y.; Xiao, Y.; et al. Isolated left ventricular noncompaction: Clinical profile and prognosis in 106 adult patients. Heart

Vessel. 2014, 29, 645–652.

22. Peters, F.; Khandheria, B.K.; dos Santos, C.; Matioda, H.; Maharaj, N.; Libhaber, E.; Mamdoo, F.; Essop, M.R. Isolated left ventricular noncompaction in sub-Saharan Africa: A clinical and echocardiographic perspective. Circ. Cardiovasc. Imaging. 2012, 5, 187–193.
23. Oechslin, E.N.; Attenhofer Jost, C.H.; Rojas, J.R.; Kaufmann, P.A.; Jenni, R. Long-term follow-up of 34 adults with isolated left ventricular noncompaction: A distinct cardiomyopathy with poor prognosis. J. Am. Coll. Cardiol. 2000, 36, 493–500.
24. Jenni, R.; Wyss, C.A.; Oechslin, E.N.; Kaufmann, P.A. Isolated ventricular noncompaction is associated with coronary microcirculatory dysfunction. J. Am. Coll. Cardiol. 2002, 39, 450–454.
25. Sengupta, P.P.; Mohan, J.C.; Mehta, V.; Jain, V.; Arora, R.; Pandian, N.G.; Khandheria, B.K. Comparison of echocardiographic features of noncompaction of the left ventricle in adults versus idiopathic dilated cardiomyopathy in adults. Am. J. Cardiol. 2004, 94, 389–391.
26. Nemes, A.; Caliskan, K.; Geleijnse, M.L.; Soliman, O.I.I.; Vletter, W.B.; ten Cate, F.J. Reduced regional systolic function is not confined to the noncompacted segments in noncompaction cardiomyopathy. Int. J. Cardiol. 2009, 134, 366–370.
27. Yousef, Z.R.; Foley, P.W.X.; Khadjooi, K.; Chalil, S.; Sandman, H.; Mohammed, N.U.H.; Leyva, F. Left ventricular non-compaction: Clinical features and cardiovascular magnetic resonance imaging. BMC Cardiovasc. Disord. 2009, 9, 37.
28. Lofiego, C.; Biagini, E.; Ferlito, M.; Pasquale, F.; Rocchi, G.; Perugini, E.; Leone, O.; Bracchetti, G.; Caliskan, K.; Branzi, A.; et al. Paradoxical contributions of non-compacted and compacted segments to global left ventricular dysfunction in isolated left ventricular noncompaction. Am. J. Cardiol. 2006, 97, 738–741.
29. Fazio, G.; Pipitone, S.; Iacona, M.A.; Marchì, S.; Mongiovì, M.; Zito, R.; Sutera, L.; Novo, G.; Novo, S. Evaluation of diastolic function by the tissue Doppler in children affected by non-compaction. Int. J. Cardiol. 2007, 116, 60–62.
30. Caliskan, K.; Soliman, O.I.; Nemes, A.; van Domburg, R.T.; Simoons, M.L.; Geleijnse, M.L. No relationship between left ventricular radial wall motion and longitudinal velocity and the extent and severity of noncompaction cardiomyopathy. Cardiovasc. Ultrasound 2012, 10, 9.
31. Guigui, S.A.; Horvath, S.A.; Arenas, I.A.; Mihos, C.G. Cardiac geometry, function and mechanics in left ventricular non-compaction cardiomyopathy with preserved ejection fraction. J. Echocardiogr. 2022, 20, 144–150.
32. Łuczak-Woźniak, K.; Werner, B. Left Ventricular Noncompaction-A Systematic Review of Risk Factors in the Pediatric Population. J. Clin. Med. 2021, 16, 1232.

33. Liu, J.; Li, Y.; Cui, Y.; Cao, Y.; Yao, S.; Zhou, X.; Wetzl, J.; Zeng, W.; Shi, H. Quantification of myocardial strain in patients with isolated left ventricular non-compaction and healthy subjects using deformable registration algorithm: Comparison with feature tracking. BMC Cardiovasc. Disord. 2020, 20, 400.

34. Yu, S.; Chen, X.; Yang, K.; Wang, J.; Zhao, K.; Dong, W.; Yan, W.; Su, G.; Zhano, S. Correlation between left ventricular fractal dimension and impaired strain assessed by cardiac MRI feature tracking in patients with left ventricular noncompaction and normal left ventricular ejection fraction. Eur. Radiol. 2022, 32, 2594–2603.

35. Cortés, M.; Oliva, M.R.; Orejas, M.; Navas, M.A.; Rábago, R.M.; Martínez, M.E.; Taibo, M.; Palfy, J.; Rey, M.; Farré, J. Usefulness of speckle myocardial imaging modalities for differential diagnosis of left ventricular noncompaction of the myocardium. Int. J. Cardiol. 2016, 223, 813–818.

36. Bellavia, D.; Michelena, H.I.; Martinez, M.; Pellikka, P.A.; Bruce, C.J.; Connolly, H.M.; Villarraga, H.R.; Veress, G.; Oh, J.K.; Miller, F.A. Speckle myocardial imaging modalities for early detection of myocardial impairment in isolated left ventricular non-compaction. Heart 2010, 96, 440–447.

37. Arenas, I.A.; Mihos, C.G.; DeFaria Yeh, D.; Yucel, E.; Elmahdy, H.M.; Santana, O. Echocardiographic and clinical markers of left ventricular ejection fraction and moderate or greater systolic dysfunction in left ventricular noncompaction cardiomyopathy. Echocardiography 2018, 35, 941–948.

38. Anwer, S.; Heiniger, P.S.; Rogler, S.; Erhart, L.; Cassani, D.; Kuzo, N.; Rebellius, L.; Schoenenberger-Berzins, R.; Schmid, D.; Nussbaum, S.; et al. Left ventricular mechanics and cardiovascular outcomes in non-compaction phenotype. Int. J. Cardiol. 2021, 336, 73–80.

39. Zhang, J.; Jiang, M.; Zheng, C.; Liu, H.; Guo, Y.; Yie, X.; Zhou, Z.; Zhou, X.; Xia, L.; Luo, M.; et al. Evaluation of isolated left ventricular noncompaction using cardiac magnetic resonance tissue tracking in global, regional and layer-specific strains. Sci. Rep. 2021, 11, 7183.

40. Visoiu, I.S.; Rimbas, R.C.; Nicula, A.I.; Mihaila-Baldea, S.; Magda, S.L.; Mihalcea, D.J.; Hayat, M.; Luchian, M.L.; Chitroceanu, A.M.; Vinereanu, D. Multimodality Imaging and Biomarker Approach to Characterize the Pathophysiology of Heart Failure in Left Ventricular Non-Compaction with Preserved Ejection Fraction. J. Clin. Med. 2023, 12, 3632.

41. Szűcs, A.; Kiss, A.R.; Gregor, Z.; Horváth, M.; Tóth, A.; Dohy, Z.; Szabó, L.E.; Suhai, F.I.; Merkely, B.; Vágó, H. Changes in strain parameters at different deterioration levels of left ventricular function: A cardiac magnetic resonance feature-tracking study of patients with left ventricular noncompaction. Int. J. Cardiol. 2021, 331, 124–130.

42. Qiu, Q.; Chen, Y.X.; Mai, J.T.; Yuan, W.L.; Wei, Y.L.; Liu, Y.M.; Yang, L.; Wang, J.F. Effects of cardiac resynchronization therapy on left ventricular remodeling and dyssynchrony in patients with left ventricular noncompaction and heart failure. Int. J. Cardiovasc. Imaging 2015, 31, 329–337.

43. Cerar, A.; Jaklic, M.; Frljak, S.; Poglajen, G.; Zemljic, G.; Salobir, B.G.; Novak, M.D.; Stalc, M.; Zbacnik, R.; Kozelj, M. Impairment of myocardial perfusion correlates with heart failure severity in patients with non-compaction cardiomyopathy. ESC Heart Fail. 2020, 7, 1161–1167.
44. Kalapos, A.; Domsik, P.; Forster, T.; Nemes, A. Left ventricular strain reduction is not confined to the noncompacted segments in noncompaction cardiomyopathy-insights from the three-dimensional speckle tracking echocardiographic MAGYAR-Path Study. Echocardiography 2014, 31, 638–643.
45. Bogunovic, N.; Farr, M.; Pirl, L.; Faber, L.; van Buuren, F.; Rudolph, V.; Roder, F. Systolic longitudinal global and segmental myocardial mechanics in symptomatic isolated left ventricular non-compaction cardiomyopathy. Echocardiography 2021, 38, 555–567.
46. Gastl, M.; Gotschy, A.; Polacin, M.; Vishnevskiy, V.; Meyer, D.; Sokolska, J.; Tanner, F.C.; Alkadhi, H.; Kozerke, S.; Manka, R. Determinants of myocardial function characterized by CMR-derived strain parameters in left ventricular non-compaction cardiomyopathy. Sci. Rep. 2019, 9, 15882.
47. Huttin, O.; Venner, C.; Frikha, Z.; Voilliot, D.; Marie, P.Y.; Aliot, E.; Sadoul, N.; Juillière, Y.; Brembilla-Perrot, B.; Selton-Suty, C. Myocardial deformation pattern in left ventricular non-compaction: Comparison with dilated cardiomyopathy. Int. J. Cardiol. Heart Vasc. 2014, 5, 9–14.
48. Akhan, O.; Demir, E.; Dogdus, M.; Cakan, F.O.; Nalbantgil, S. Speckle tracking echocardiography and left ventricular twist mechanics: Predictive capabilities for noncompaction cardiomyopathy in the first degree relatives. Int. J. Cardiovasc. Imaging 2021, 37, 429–438.
49. Zhou, D.; Li, S.; Sirajuddin, A.; Wu, W.; Huang, J.; Sun, X.; Zhao, S.; Pu, J.; Lu, M. CMR Characteristics, gene variants and long-term outcome in patients with left ventricular non-compaction cardiomyopathy. Insights Imaging 2021, 12, 184.
50. Kiss, A.R.; Gregor, Z.; Furák, A.; Tóth, A.; Horváth, M.; Szabó, L.; Czimbalmos, C.; Dohy, Z.; Merkely, B.; Vágó, H.; et al. Left ventricular characteristics of noncompaction phenotype patients with good ejection fraction measured with cardiac magnetic resonance. Anatol. J. Cardiol. 2021, 25, 565–571.
51. Sarnecki, J.; Paszkowska, A.; Petryka-Mazurkiewicz, J.; Kubik, A.; Feber, J.; Jurkiewicz, E.; Ziółkowska, E. Left and Right Ventricular Morphology, Function and Myocardial Deformation in Children with Left Ventricular Non-Compaction Cardiomyopathy: A Case-Control Cardiovascular Magnetic Resonance Study. J. Clin. Med. 2022, 11, 1104.
52. Koh, C.; Hong, W.J.; Wong, S.J.; Cheung, Y.F. Systolic-diastolic coupling of myocardial deformation of the left ventricle in children with left ventricular noncompaction. Heart Vessels 2010, 25, 493–499.
53. Ari, M.E.; Cetin, I.I.; Kocabas, A.; Ekici, F.; Ceylan, O.; Surucu, M. Decreased Deformation in Asymptomatic Children with Isolated Left Ventricular Non-compaction and Normal Ejection

Fraction. Pediatr. Cardiol. 2016, 37, 201–207.

54. Yubbu, P.; Nawaytou, H.M.; Calderon-Anyosa, R.; Banerjee, A. Diagnostic value of myocardial deformation pattern in children with noncompaction cardiomyopathy. Int. J. Cardiovasc. Imaging 2018, 34, 1529–1539.
55. Nucifora, G.; Raman, K.S.; Muser, D.; Shah, R.; Perry, R.; Ramli, K.A.A.; Selvanayagam, J.B. Cardiac magnetic resonance evaluation of left ventricular functional, morphological, and structural features in children and adolescents vs. young adults with isolated left ventricular non-compaction. Int. J. Cardiol. 2017, 246, 68–73.
56. Arunamata, A.; Stringer, J.; Balasubramanian, S.; Tacy, T.A.; Silverman, N.H.; Punn, R. Cardiac Segmental Strain Analysis in Pediatric Left Ventricular Noncompaction Cardiomyopathy. J. Am. Soc. Echocardiogr. 2019, 32, 763–773.e1.
57. Zheng, T.; Ma, X.; Li, S.; Ueda, T.; Wang, Z.; Lu, A.; Zhou, W.; Zou, H.; Zhao, L.; Gong, L. Value of Cardiac Magnetic Resonance Fractal Analysis Combined with Myocardial Strain in Discriminating Isolated Left Ventricular Noncompaction and Dilated Cardiomyopathy. J. Magn. Reson. Imaging 2019, 50, 153–163.
58. Tarando, F.; Coisne, D.; Galli, E.; Rousseau, C.; Viera, F.; Bosseau, C.; Habib, G.; Lederlin, M.; Schnell, F.; Donal, E. Left ventricular non-compaction and idiopathic dilated cardiomyopathy: The significant diagnostic value of longitudinal strain. Int. J. Cardiovasc. Imaging 2017, 33, 83–95.
59. Niemann, M.; Liu, D.; Hu, K.; Cikes, M.; Beer, M.; Herrmann, S.; Gaudron, P.D.; Hillenbrand, H.; Voelker, W.; Ertl, G.; et al. Echocardiographic quantification of regional deformation helps to distinguish isolated left ventricular non-compaction from dilated cardiomyopathy. Eur. J. Heart Fail. 2012, 14, 155–161.
60. Gregor, Z.; Kiss, A.R.; Grebur, K.; Szabó, L.E.; Merkely, B.; Vágó, H.; Szűcs, A. MR-specific characteristics of left ventricular noncompaction and dilated cardiomyopathy. Int. J. Cardiol. 2022, 359, 69–75.
61. Zhu, L.; Wu, J.; Hao, X.; Li, X. Value of cardiac magnetic resonance feature tracking technology in the differential diagnosis of isolated left ventricular noncompaction and dilated cardiomyopathy. Quant. Imaging Med. Surg. 2023, 13, 1453–1463.
62. Haland, T.F.; Saberniak, J.; Leren, I.S.; Edvardsen, T.; Haugaa, K.H. Echocardiographic comparison between left ventricular non-compaction and hypertrophic cardiomyopathy. Int. J. Cardiol. 2017, 228, 900–905.
63. Ashwal, A.J.; Mugula, S.R.; Samanth, J.; Paramasivam, G.; Nayak, K.; Padmakumar, R. Role of deformation imaging in left ventricular non-compaction and hypertrophic cardiomyopathy: An Indian perspective. Egypt. Heart J. 2020, 72, 6.

64. Zou, Q.; Xu, R.; Li, X.; Yu, H.Y.; Yang, Z.G.; Wang, Y.N.; Fan, H.M.; Guo, Y.K. The mitral regurgitation effects of cardiac structure and function in left ventricular noncompaction. Sci. Rep. 2021, 11, 4616.

65. Wang, J.X.; Li, X.; Xu, R.; Hou, R.L.; Yang, Z.G.; Zhou, Z.Q.; Wang, Y.N.; Guo, Y.K. Comparison of cardiovascular magnetic resonance features and clinical consequences in patients with left ventricular non-compaction with and without mitral regurgitation-a multi-institutional study of the retrospective cohort study. Cardiovasc. Diagn. Ther. 2022, 12, 241–252.

66. Dorobantu, D.M.; Radulescu, C.R.; Riding, N.; McClean, G.; de la Garza, M.S.; Abuli-LLuch, M.; Duarte, N.; Adamuz, M.C.; Ryding, D.; Perry, D.; et al. The use of 2-D speckle tracking echocardiography in assessing adolescent athletes with left ventricular hypertrabeculation meeting the criteria for left ventricular non-compaction cardiomyopathy. Int. J. Cardiol. 2023, 371, 500–507.

67. Sabatino, J.; Di Salvo, G.; Krupickova, S.; Fraisse, A.; Prota, C.; Bucciarelli, V.; Josen, M.; Paredes, J.; Sirico, D.; Voges, I.; et al. Left Ventricular Twist Mechanics to Identify Left Ventricular Noncompaction in Childhood. Circ. Cardiovasc. Imaging 2019, 12, e007805.

68. Peters, F.; Khandheria, B.K.; Libhaber, E.; Maharaj, N.; Dos Santos, C.; Matioda, H.; Essop, M.R. Left ventricular twist in left ventricular noncompaction. Eur. Heart J. Cardiovasc. Imaging 2014, 15, 48–55.

69. Van Dalen, B.M.; Caliskan, K.; Soliman, O.I.I.; Nemes, A.; Vletter, W.B.; Ten Cate, F.J.; Geleijnse, M.L. Left ventricular solid body rotation in non-compaction cardiomyopathy: A potential new objective and quantitative functional diagnostic criterion? Eur. J. Heart Fail. 2008, 10, 1088–1093.

70. Van Dalen, B.M.; Caliskan, K.; Soliman, O.I.I.; Kauer, F.; van der Zwaan, H.B.; Vletter, W.B.; van Kark, L.C.; Ten Cate, F.J.; Geleijnse, M.L. Diagnostic Value of Rigid Body Rotation in Noncompaction Cardiomyopathy. J. Am. Soc. Echocardiogr. 2011, 24, 548–555.

71. Nawaytou, H.M.; Montero, A.E.; Yubbu, P.; Calderón-Anyosa, R.J.C.; Sato, T.; O'Connor, M.J.; Miller, K.D.; Ursell, P.C.; Hoffman, J.I.E.; Banerjee, A. A Preliminary Study of Left Ventricular Rotational Mechanics in Children with Noncompaction Cardiomyopathy: Do They Influence Ventricular Function? J. Am. Soc. Echocardiogr. 2018, 31, 951–961.

72. Peters, F.; Khandheria, B.K.; dos Santos, C.; Govender, S.; Botha, F.; Essop, M.R. Peripartum Cardiomyopathy Associated with Left Ventricular Noncompaction Phenotype and Reversible Rigid Body Rotation. Circ. Heart Fail. 2013, 6, e62–e63.

73. Lang, R.M.; Badano, L.P.; Mor-Avi, V.; Afilalo, J.; Armstrong, A.; Ernande, L.; Flachskampf, F.A.; Foster, E.; Goldstein, S.A.; Kuznetsova, T.; et al. Recommendations for cardiac chamber quantification by echocardiography in adults: An update from the American Society of Echocardiography and the European Association of Cardiovascular Imaging. Eur. Heart J. Cardiovasc. Imaging 2015, 16, 233–270.

74. Hoit, B.D. Left atrial size and function: Role in prognosis. J. Am. Coll. Cardiol. 2014, 63, 493–505.
75. Badano, L.P.; Nour, A.; Muraru, D. Left atrium as a dynamic three-dimensional entity: Implications for echocardiographic assessment. Rev. Esp. Cardiol. 2013, 66, 1–4.
76. Xu, W.; Yang, Y.; Zhu, J.; Tan, J.; Wang, J.; Wang, L. Left Atrial Diameter and the Risk of Thromboembolism in Patients with Left Ventricular Noncompaction. J. Cardiovasc. Dev. Dis. 2022, 9, 426.
77. Nemes, A.; Anwar, A.M.; Caliskan, K.; Soliman, O.I.I.; van Dalen, B.M.; Geleijnse, M.L.; ten Cate, F.J. Evaluation of left atrial systolic function in noncompaction cardiomyopathy by real-time three-dimensional echocardiography. Int. J. Cardiovasc. Imaging 2008, 24, 237–242.
78. Nemes, A.; Piros, G.Á.; Domsik, P.; Kalapos, A.; Forster, T. Left Atrial Volumetric and Strain Analysis by Three-Dimensional Speckle-Tracking Echocardiography in Noncompaction Cardiomyopathy: Results from the MAGYAR-Path Study. Hell. J. Cardiol. 2016, 57, 23–29.
79. Han, P.L.; Shen, M.T.; Jiang, Y.; Jiang, Z.K.; Li, K.; Yang, Z.G. Prognostic Value of Left Atrial Reservoir Strain in Left Ventricular Myocardial Noncompaction: A 3.0 T Cardiac Magnetic Resonance Feature Tracking Study. J. Magn. Reson. Imaging 2023, 57, 559–575.
80. Dal-Bianco, J.P.; Levine, R.A. Anatomy of the mitral valve apparatus: Role of 2D and 3D echocardiography. Cardiol. Clin. 2013, 31, 151–164.
81. Silbiger, J.J.; Bazaz, R. The anatomic substrate of mitral annular contraction. Int. J. Cardiol. 2020, 306, 158–161.
82. Mihaila, S.; Muraru, D.; Miglioranza, M.H.; Piasentini, E.; Peluso, D.; Cucchini, U.; Iliceto, S.; Vinereanu, D.; Badano, L.P. Normal mitral annulus dynamics and its relationships with left ventricular and left atrial function. Int. J. Cardiovasc. Imaging 2015, 31, 279–290.
83. Nemes, A.; Anwar, A.M.; Caliskan, K.; Soliman, O.I.I.; van Dalen, B.M.; Geleijnse, M.L.; ten Cate, F.J. Non-compaction cardiomyopathy is associated with mitral annulus enlargement and functional impairment: A real-time three-dimensional echocardiographic study. J. Heart Valve Dis. 2008, 17, 31–35.
84. Nemes, A.; Rácz, G.; Kormányos, Á. Tricuspid Annular Abnormalities in Isolated Left Ventricular Non-compaction-Insights From the Three-dimensional Speckle-Tracking Echocardiographic MAGYAR-Path Study. Front. Cardiovasc. Med. 2022, 9, 694616.
85. Li, Q.; Miao, L.; Xia, L.; Abdelnasser, H.Y.; Zhang, F.; Lu, Y.; Nusrat, A.; Tabassum, M.; Li, J.; Wu, M. Left Ventricular Noncompaction Is Associated with Valvular Regurgitation and a Variety of Arrhythmias. J. Cardiovasc. Dev. Dis. 2022, 9, 49.
86. Vahanian, A.; Beyersdorf, F.; Praz, F.; Milojevic, M.; Baldus, S.; Bauersachs, J.; Capodanno, D.; Conradi, L.; De Bonis, M.; De Paulis, R.; et al. 2021 ESC/EACTS Guidelines for the management

of valvular heart disease. Eur. Heart J. 2022, 43, 561–632.

87. Zhang, D.; Lu, Y.T.; Zhou, Z.M.; Hu, Y.X.; Liu, X.C.; Qu, Y.; Liu, Y.X.; Liu, Y.X.; Zhou, X.L. Clinical characteristics and management of coexistent cardiomyopathy in patients with bicuspid aortic valve. J. Geriatr. Cardiol. 2023, 20, 205–213.
88. Jeong, H.; Shim, C.Y.; Kim, D.; Choi, J.Y.; Choi, K.U.; Lee, S.Y.; Hong, G.R.; Ha, J.W. Prevalence, Characteristics, and Clinical Significance of Concomitant Cardiomyopathies in Subjects with Bicuspid Aortic Valves. Yonsei Med. J. 2019, 60, 816–823.
89. Agarwal, A.; Khandheria, B.K.; Paterick, T.E.; Treiber, S.C.; Bush, M.; Tajik, A.J. Left ventricular noncompaction in patients with bicuspid aortic valve. J. Am. Soc. Echocardiogr. 2013, 26, 1306–1313.
90. Shen, M.; Capoulade, R.; Tastet, L.; Guzzetti, E.; Clavel, M.A.; Salaun, E.; Bédard, É.; Arsenault, M.; Chetaille, P.; Tizón-Marcos, H.; et al. Prevalence of left ventricle non-compaction criteria in adult patients with bicuspid aortic valve versus healthy control subjects. Open Heart 2018, 5, e000869.
91. Shim, C.Y. Arterial-cardiac interaction: The concept and implications. J. Cardiovasc. Ultrasound 2011, 19, 62–66.
92. Belz, G.G. Elastic properties and Windkessel function of the human aorta. Cardiovasc. Drugs Ther. 1995, 9, 73–83.
93. Tukker, M.; Leening, M.J.G.; Mohamedhoesein, S.; Vanmaele, A.L.A.; Caliskan, K. Prevalence and clinical correlates of ascending aortic dilatation in patients with noncompaction cardiomyopathy. Int. J. Cardiovasc. Imaging 2023, 39, 1687–1695.
94. Nemes, A.; Caliskan, K.; Geleijnse, M.L.; Soliman, O.I.I.; Anwar, A.M.; ten Cate, F.J. Alterations in aortic elasticity in noncompaction cardiomyopathy. Int. J. Cardiovasc. Imaging 2008, 24, 7–13.
95. Foale, R.; Nihoyannopoulos, P.; McKenna, W.; Kleinebenne, A.; Nadazdin, A.; Rowland, E.; Smith, G. Echocardiographic measurement of the normal adult right ventricle. Br. Heart J. 1986, 56, 33–44.
96. Ho, S.Y.; Nihoyannopoulos, P. Anatomy, echocardiography, and normal right ventricular dimensions. Heart 2006, 92 (Suppl. 1), i2–i13.
97. Haddad, F.; Hunt, S.A.; Rosenthal, D.N.; Murphy, D.J. Right ventricular function in cardiovascular disease, Part I. Anatomy, physiology, aging, and functional assessment of the right ventricle. Circulation 2008, 117, 1436–1448.
98. Rudski, L.G.; Lai, W.W.; Afilalo, J.; Hua, L.; Handschumacher, M.D.; Chandrasekaran, K.; Solomon, S.D.; Louie, E.K.; Schiller, N.B. Guidelines for the echocardiographic assessment of the right heart in adults: A report from the American Society of Echocardiography endorsed by the

European Association of Echocardiography, a registered branch of the European Society of Cardiology, and the Canadian Society of Echocardiography. J. Am. Soc. Echocardiogr. 2010, 23, 685–713.

99. Stacey, R.B.; Andersen, M.; Haag, J.; Hall, M.E.; McLeod, G.; Upadhya, B.; Hundley, W.G.; Thohan, V. Right ventricular morphology and systolic function in left ventricular noncompaction cardiomyopathy. Am. J. Cardiol. 2014, 113, 1018–1023.
100. Nucifora, G.; Aquaro, G.D.; Masci, P.G.; Pingitore, A.; Lombardi, M. Magnetic resonance assessment of prevalence and correlates of right ventricular abnormalities in isolated left ventricular noncompaction. Am. J. Cardiol. 2014, 113, 142–146.
101. Stämpfli, S.F.; Gotschy, A.; Kiarostami, P.; Özkartal, T.; Gruner, C.; Niemann, M.; Manka, R.; Tanner, F.C. Right ventricular involvement in left ventricular non-compaction cardiomyopathy. Cardiol. J. 2022, 29, 454–462.
102. Gregor, Z.; Kiss, A.R.; Grebur, K.; Dohy, Z.; Kovács, A.; Merkely, B.; Vágó, H.; Szűcs, A. Characteristics of the right ventricle in left ventricular noncompaction with reduced ejection fraction in the light of dilated cardiomyopathy. PLoS ONE 2023, 18, e0290981.
103. Kiss, A.R.; Gregor, Z.; Popovics, A.; Grebur, K.; Szabó, L.E.; Dohy, Z.; Kovács, A.; Lakatos, B.K.; Merkely, B.; Vágó, H.; et al. Impact of Right Ventricular Trabeculation on Right Ventricular Function in Patients with Left Ventricular Non-compaction Phenotype. Front. Cardiovasc. Med. 2022, 9, 843952.
104. Leung, S.W.; Elayi, C.S.; Charnigo Jr, R.J.; Syed, M.A. Clinical significance of right ventricular dysfunction in left ventricular non-compaction cardiomyopathy. Int. J. Cardiovasc. Imaging 2012, 28, 1123–1131.
105. Wang, W.; Chen, W.; Lin, X.; Fang, L. Influence of Right Ventricular Dysfunction on Outcomes of Left Ventricular Non-compaction Cardiomyopathy. Front. Cardiovasc. Med. 2022, 9, 816404.
106. Tadic, M. The right atrium, a forgotten cardiac chamber: An updated review of multimodality imaging. J. Clin. Ultrasound 2015, 43, 335–345.
107. Nemes, A.; Domsik, P.; Kalapos, A.; Gavallér, H.; Oszlánczi, M.; Forster, T. Right atrial deformation analysis in isolated left ventricular noncompaction–insights from the three-dimensional speckle tracking echocardiographic MAGYAR-Path Study. Rev. Port. Cardiol. 2016, 35, 515–521.
108. Dahou, A.; Levin, D.; Reisman, M.; Hahn, R.T. Anatomy and physiology of the tricuspid valve. JACC Cardiovasc. Imaging 2019, 12, 458–468.
109. Kivelitz, D.E.; Dohmen, P.M.; Lembcke, A.; Kroencke, T.J.; Klingebiel, R.; Hamm, B.; Konertz, W.; Taupitz, M. Visualization of the pulmonary valve using cine MR imaging. Acta Radiol. 2003, 44, 172–176.

110. Hirono, K.; Ichida, F. Left ventricular noncompaction: A disorder with genotypic and phenotypic heterogeneity-a narrative review. Cardiovasc. Diagn. Ther. 2022, 12, 495–515.
111. van Waning, J.I.; Moesker, J.; Heijsman, D.; Boersma, E.; Majoor-Krakauer, D. Systematic Review of Genotype-Phenotype Correlations in Noncompaction Cardiomyopathy. J. Am. Heart. Assoc. 2019, 8, e012993.
112. Marakhonov, A.V.; Brodehl, A.; Myasnikov, R.P.; Sparber, P.A.; Kiseleva, A.V.; Kulikova, O.V.; Meshkov, A.N.; Zharikova, A.A.; Koretsky, S.N.; Kharlap, M.S.; et al. Noncompaction cardiomyopathy is caused by a novel in-frame desmin (DES) deletion mutation within the 1A coiled-coil rod segment leading to a severe filament assembly defect. Hum. Mutat. 2019, 40, 734–741.
113. Kulikova, O.; Brodehl, A.; Kiseleva, A.; Myasnikov, R.; Meshkov, A.; Stanasiuk, C.; Gärtner, A.; Divashuk, M.; Sotnikova, E.; Koretskiy, S.; et al. The Desmin (DES) Mutation p.A337P Is Associated with Left-Ventricular Non-Compaction Cardiomyopathy. Genes 2021, 12, 121.
114. My, I.; Di Pasquale, E. Genetic Cardiomyopathies: The Lesson Learned from hiPSCs. J. Clin. Med. 2021, 10, 1149.
115. Purevjav, E.; Chintanaphol, M.; Orgil, B.O.; Alberson, N.R.; Towbin, J.A. Left ventricular noncompaction cardiomyopathy: From clinical features to animal modeling. In Preclinical Animal Modeling in Medicine, 1st ed.; Purevjav, E., Pierre, J.F., Lu, L., Eds.; IntechOpen: London, UK, 2022.